EXPERIMENTAL RESEARCH ON OFF-DESIGN CHARACTERISTICS OF HEAT PUMP WATER HEATER USING LOW GWP ZEOTROPIC BLEND

Fujun JU[1*], Wenbo LIU[1], Zhenzhen MU[1], Xiaowei FAN[1,2], Huifan ZHENG[1],

Lihao HOU[1], and Qinglei LIU[1]

[*1] School of Smarts Energy and Environment, Zhongyuan University of Technology, Zhengzhou 450007, China

[2] School of Energy and Building Environment Engineering, Henan University of Urban Construction, Pingdingshan 467036, China

[*] Corresponding author; E-mail: jufujun2008@163.com

Based on the test setup of instant heat pump water heater (IHPWH), the performances of system operating with zeotropic natural mixture (ZNM) (R744/R290 (12/88)) and system operating with R22 refrigerant were compared under variable entry temperature of heat sink (ETHSK) and variable entry temperature of heat source (ETHSC) conditions, aiming to comprehensively evaluate the replacement potential of ZNM in the IHPWH. The results revealed that ZNM had an obvious alternative advantage, mainly attributed to that system operating with ZNM refrigerant achieved the comparable or markedly superior heating capacity and COP and markedly lower discharge temperature compared to those of system operating with R22 refrigerant under two conditions. The discharge temperature of system operating with ZNM refrigerant was reduced by 5.4~26.7 ℃ compared to that of system operating with R22 refrigerant, thus system operating with ZNM refrigerant can produce higher temperature domestic hot water. Compared with those of system operating with R22 refrigerant, both heating capacity and COP of system operating with ZNM refrigerant had markedly different trends with the change of ETHSK, while they had slightly different trends with the change of ETHSC. Compared to the ETHSK, the ETHSC has a more conspicuous impact on the heating capacity, COP and discharge temperature of system operating with ZNM refrigerant.

Key words: *Off-design performances, Refrigerant substitution, Zeotropic natural mixture, R744/R290, Heat pump water heater*

1. Introduction

Heat pump technology has been effectively promoted and applied in the domestic hot water production and heating by virtue of its highly efficient and energy saving advantages [1,2]. Considering the environmental impact of global warming owing to the use of high GWP refrigerants, the search for eco-friendly alternative refrigerants has become the research hotspot in the heat pumps field. In particular, the issue of the Kigali Amendment has accelerated the elimination of high GWP refrigerants [3]. Zeotropic blends can realize the complementary advantages between binary or multiple

components, and its temperature slip helps to improve the temperature matching performance of the heat transfer process and improve the energy efficiency of the system, so they have become the main way to find efficient green alternative refrigerants.

The alternative performance of HFCs/HCs in heat pump systems has been evaluated by many scholars. The theoretical research of Yu et al. [4] showed that the *COP* of transcritical high temperature heat pump water heater with R32/R290 (70/30) was increased by 10.2%~23.7% compared with that of R744 system. The test research of Tian et al. [5] indicated that the heating capacity of heat pump air conditioner with R32/R290 (68/32) was improved by 6.1%~16.4% compared with that of R410A system. The theoretical study of Wang et al. [6] revealed that both instant heat pump water heater (IHPWH) systems with R125/R600 (30/70) and R125/R600a (30/70) obtained the higher *COP* than that of R22 system.

Many scholars have conducted the research on the substitution potential of HFOs/HCs in heat pump systems. The test research of Sieres et al. [7] indicated that heating heat pump with R32/R1234yf (68.9/31.1) achieved comparable *COP* compared to that of R410A system. The test study of Fukuda et al. [8] revealed that heating heat pump with R32/R1234ze(E) (80/20) obtained the maximum *COP*. The theoretical research of Wang et al. [9] showed that the *COP* of IHPWH with R32/R1234ze (70/30) was higher than that of R410A system.

The substitution performances of R744/HCs blends were investigated in heat pumps because of the advantages of low GWP and good thermophysical properties. The theoretical study of Yu et al. [10] showed that autocascade heat pump with R744/R290 (80/20) had marked advantages over R744 system under low temperature condition. Luo et al. [11,12] found in the theoretical and experimental research that R744/R600a was the applicable refrigerant in the novel compound heating heat pump in cold regions. Liu et al. [13] theoretically evaluated the suitability of 15 low GWP non-azeotropic mixtures (such as R744/R290, R744/RE170 etc.) used in the IHPWH and revealed that *COP* of R744/RE170 (30/70) was superior to other blends. The test research of Zhang et al. [14] revealed that transcritical IHPWH with R744/R290 (78/22) obtained the highest *COP*. Dai et al. [15] analyzed the feasibility of applying R744/HCs to the heat pump drying system and indicated that R744/RE170 (60/40) obtained higher *COP* than other mixtures at the operating condition. The test and simulation study of Ju et al. [16,17] revealed that the *COP* and heating capacity of IHPWH system with ZNM (R744/R290 (12/88)) were obviously superior to that of R22 IHPWH system under nominal condition and variable outlet temperature of heat sink (OTHSK) conditions.

The study on off-design performances is necessary for fully evaluating the substitution potential of refrigerants. Cui et al. [18] theoretically analyzed the influence of entry temperature of heat sink (ETHSK) and OTHSK on the performance of R744 transcritical IHPWH system and found that R744 systems significantly dominated the *COP* and heat transfer matching performance over R134a systems under low ETHSK condition and large heat sink temperature rise condition. Pitarch et al. [19] tested the effect of subcooling on the *COP* of IHPWH system with R290 and indicated that the *COP* of IHPWH system by making subcooling was higher 31% compared to that without subcooling under the nominal condition. Pitarch et al. [20] varied the heat sink and heat source operating parameters to obtain the optimal superheat and subcooling of IHPWH system with R290 based on the simulation model and revealed that the IHPWH system achieved up to a 23% increase in *COP* under the optimal subcooling and superheat conditions.

HFCs/HCs, HFOs/HCs and R744/HCs all showed promising alternative potential in heat pump systems, but HFCs and HFOs are synthetic refrigerants, and their production process requires a lot of energy consumption and carbon emissions. At the same time, HFCs still has a high GWP, and HFOs is not only expensive, but also produces hydrogen fluoride and trifluoroacetic acid in its production and degradation process, causing damage to the environment and even endangering human health. Thus, R744/HCs was selected as the research object in this study.

A comprehensive evaluation of the substitution properties of candidate refrigerants is the only way to reasonably judge their substitution potential. In our previous study, we have completed the concentration optimization of R744/R290 with large temperature slip and the preliminary evaluation of its substitution performance in IHPWH system with the high heat sink temperature rise through the comparative analysis of the system performances under nominal condition and variable OTHSK conditions, but the comprehensive evaluation of its substitution performance is still lacking. Thus, on the basis of our previous research [16,17], the impacts of ETHSK and entry temperature of heat source (ETHSC) on the performances of R744/R290 (12/88) (referred to as ZNM) IHPWH system and R22 IHPWH system were experimentally investigated and compared by using the self-built IHPWH test device, with the aim of comprehensive evaluation of the replacement potential of ZNM in the IHPWH system and providing a reference for the promotion of low GWP zeotropic mixtures with large temperature slip.

2. Materials and Methods

2.1. IHPWH test rig

As exhibited in Fig. 1, the IHPWH test rig used to compare the performances of systems operating with ZNM refrigerant and R22 refrigerant under variable conditions consisted of two main components: the IHPWH unit and the data acquisition system. The IHPWH unit mainly had the fixed frequency compressor, contra-flow casing type condenser, contra-flow casing type evaporator, throttling device, cooling water tank and heating water tank etc. The compressor was a R22 compressor using 4GS mineral oil with a displacement of 3.798 m^3/h and the maximum allowable discharge temperature of 110 ℃, which was designed for heat pump water heaters. The inner tubes of heat exchangers were purple copper smooth tubes and their outer tubes were brass smooth tubes, and the refrigerant (ZNM or R22) flowed in the inner tubes, and the heat source and heat sink flowed in the corresponding channel rings. The tube lengths of the condenser and the evaporator were 21.6 m and 9.6 m respectively. And the detailed structure dimensions of them were listed in Tab. 1. The throttling device was a manual throttle valve, and its maximum allowable working temperature and working pressure were 100 ℃ and 20.0 MPa respectively. The cooling water tank and the heating water tank were both constant temperature tanks with an accuracy of 0.1 ℃, and the refrigeration unit and the heaters were installed inside them respectively, which could ensure the requirement of heat sink and heat source at different temperatures. A filter dryer was installed in front of the throttle valve to absorb water vapor and filter other impurities from the system to prevent ice clogging and damage to other components.

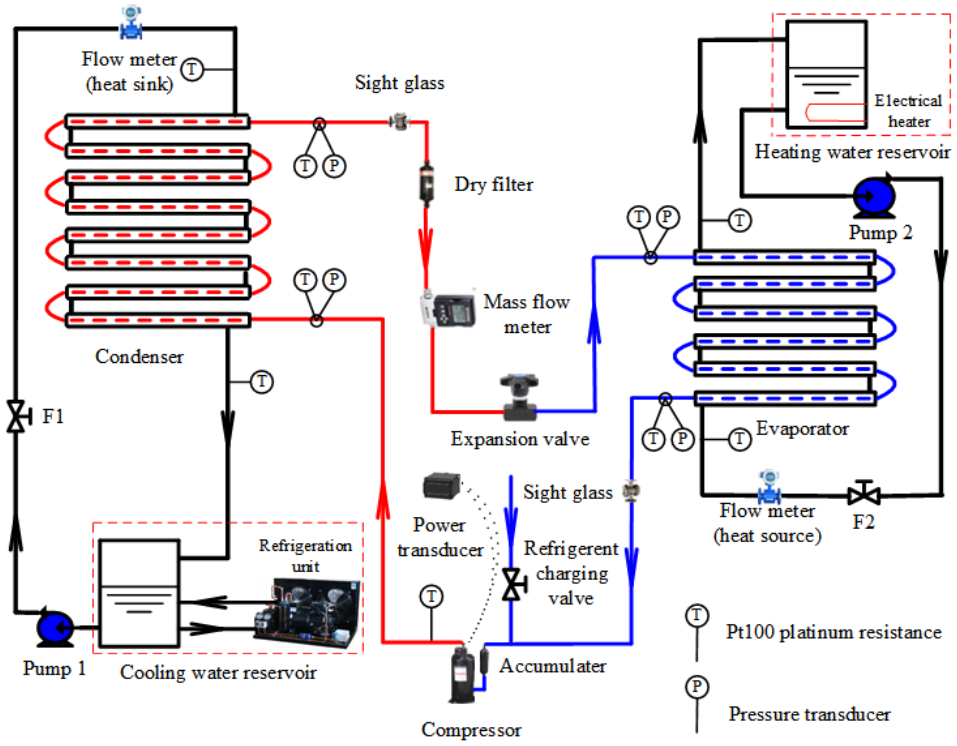

Figure 1. Layout of the test rig for IHPWH.

Table 1. Dimensions of the inner tube and outer tubes.

Type	Outer Tube Outer Diameter/mm	Outer Tube Wall Thickness/mm	Inner Tube Outer Diameter/mm	Inner Tube Wall Thickness/mm
Evaporator	22	1	12.7	0.75
Condenser	16	1.5	9.52	0.8

Fig. 1 shows the layouts of the measuring instruments and the measurement points. The detailed information about measurement accuracies, ranges and model of measuring instruments used in the test were illustrated in Tab. 2. The Pt100 platinum resistances, calibrated by a thermocouple calibrator, were used to measure the temperatures of the refrigerant and secondary fluids at the key positions. The pressure sensors, mass flow meter, power transmitter and electromagnetic flow meters were calibrated by professional institutions before the test. The ranges of the pressure sensors can be adjusted by the manufacturer according to the needs of the test. The differences in measuring range and measuring accuracy of the two electromagnetic flow meters were caused by the difference in the diameter of their internal measuring tubes. A Keithley 2700 data acquisition instrument was used for real-time and automated continuous collection and storage of all directly measured parameters.

Table 2. Detailed information of measuring instruments.

Parameters	Measuring Instrument	Brand/Model	Scope	Precision
Temperature	Pt100	Omron/Level A	-200~650 ℃	0.1 ℃
Pressure	Pressure sensor	Rosemount/3051TA	0~4.0 MPa	0.04%
		Rosemount/3051TA	0~2.0 MPa	0.04%
Refrigerant flow rate	Mass flow meter	Siemens/MASS 2100 sensor and MASS 6000 transmitter	0~140 kg·h^{-1}	0.1%

Power	Power transmitter	Shanghai Yadu Electronic Technology Co., LTD/ Customization	0~3.0 kW	0.5%
Heat sink flow rate	Electromagnetic flow meter	Siemens/MAG 1100 sensor and MAG 6000 transmitter	0~160 kg·h^{-1}	0.2%
Heat source flow rate	Electromagnetic flow meter	Siemens/MAG 1100 sensor and MAG 6000 transmitter	0~1080 kg·h^{-1}	0.25%
Refrigerant charge	Electronic platform scale	Qingdao Yuheng weighing equipment Co., LTD/ Customization	0~15 kg	0.1 g

2.2. Experimental conditions

In order to further evaluate the potential of ZNM to replace R22 in the IHPWH system, the environmental side parameters of test conditions were set (shown in Tab. 3) based on GB/T23137-2020 [21] and literature [16], in which the heat source flow was obtained from the experiment study of nominal condition performance. According to the literature [16], considering the large temperature glide of ZNM, the same method as literature [16] and [22] was adopted to set the temperature of ZNM at the entrance of evaporator as the ETHSC decreased by 20 ℃, and the temperature of R22 at the entrance of evaporator (evaporation temperature) as the ETHSC decreased by 10 ℃. This means that the evaporation temperature (the arithmetic means of the refrigerants temperature at the evaporator inlet and the dew point temperature) of ZNM was no greater than the evaporation temperature of R22 under the same test condition, further enhancing the reliability of the evaluation of the substitution potential of ZNM. The ETHSK and ETHSC were adjusted by changing the temperature settings of the cooling water tank and the heating water tank. The OTHSK and heat source flow rate required by the test can be obtained by changing the openings of the corresponding regulating valves.

Table 3. Environmental side parameters of test conditions.

Working Condition Types	t_{ski}/℃	t_{sko}/℃	t_{sci}/℃	M_{sc}/kg·s^{-1}
Nominal condition	15	55	20	0.178
Variable ETHSK condition	10~20	55	20	0.178
Variable ETHSC condition	15	55	10~30	0.178

In order to minimize heat loss between the test facility and the laboratory air environment, the heat exchangers, mass flow meter, connecting pipes and other components were equipped with adequate thickness of thermal insulation foam. An inverter room air conditioner was used to maintain the laboratory air dry bulb temperature at 20 ± 1.5 ℃ to reduce the influence of heat loss between the test equipment and the laboratory air environment on the experimental results. The time interval of teat data acquisition was set to 20 s. When the changes of the refrigerant pressures, temperatures, power and mass flow rates were within the ranges of ± 5 kPa, ± 0.2 ℃, ± 0.02 kW and ± 0.2 g·s^{-1} respectively, the IHPWH system was considered to be in a stable operating state. And then the data acquisition lasted at least 30 min.

2.3. Data processing and uncertainty analysis

The *COP* of IHPWH can be given by,

$$COP = Q_{\mathrm{h}} / W_{\mathrm{com}} \tag{1}$$

The heating capacity of IHPWH can be obtained by,

$$Q_{\mathrm{h}} = M_{\mathrm{sk}} c_{\mathrm{p}} (t_{\mathrm{sko}} - t_{\mathrm{ski}}) \tag{2}$$

The pressure ratio of IHPWH can be expressed as,

$$R_{\mathrm{com}} = P_{\mathrm{dis}} / P_{\mathrm{suc}} \tag{3}$$

The uncertainty of Q_{h} can be expressed as,

$$\frac{\Delta Q_{\mathrm{h}}}{Q_{\mathrm{h}}} = \sqrt{\left(\frac{\Delta M_{\mathrm{sk}}}{M_{\mathrm{sk}}}\right)^2 + \left(\frac{\Delta t_{\mathrm{ski}}}{t_{\mathrm{ski}}}\right)^2 + \left(\frac{\Delta t_{\mathrm{sko}}}{t_{\mathrm{sko}}}\right)^2} \tag{4}$$

The uncertainty of *COP* can be given by,

$$\frac{\Delta COP}{COP} = \sqrt{\left(\frac{\Delta Q_{\mathrm{h}}}{Q_{\mathrm{h}}}\right)^2 + \left(\frac{\Delta W_{\mathrm{com}}}{W_{\mathrm{com}}}\right)^2} \tag{5}$$

The uncertainty of Q_{h} can be expressed as,

$$\frac{\Delta R_{\mathrm{com}}}{R_{\mathrm{com}}} = \sqrt{\left(\frac{\Delta P_{\mathrm{dis}}}{P_{\mathrm{dis}}}\right)^2 + \left(\frac{\Delta P_{\mathrm{suc}}}{P_{\mathrm{suc}}}\right)^2} \tag{6}$$

The uncertainties of the indirect parameters, including heating capacity, *COP* and pressure ratio, for the system operating with ZNM refrigerant were calculated using the second power method under the nominal condition, and they were determined to be 2.79%, 3.20% and 0.46%, respectively [23].

2.4. Refrigerant charge and discharge

Before refrigerant charging, it is necessary to vacuum the system for more than 30 min to remove the non-condensing gases and some water vapor. At the same time, the air in the pipes connecting the refrigerant tank and the refrigerant charging valve must be completely discharged to prevent it from entering the system. The high precision electronic platform scale (see Tab. 2) was used to ensure the accuracy of the refrigerant charge. When ZNM was charged, the high boiling point refrigerant R290 was charged first and the low boiling point refrigerant R744 was charged later. And a refrigerant recovery machine was used to transfer the refrigerant from the system to the recovery tank during the refrigerant discharge process, to minimize the discharge of refrigerant to the atmosphere.

3. Refrigerant properties

Table 4 displays the fundamental physical and environmental characteristics of ZNM and R22. The arithmetic average of the dew point and bubble point at the standard atmospheric pressure was used as the normal boiling point of ZNM. The temperature slip shown in the table was the temperature slip of ZNM at the standard atmospheric pressure. Under the same evaporation temperature and condensation temperature conditions, a higher critical temperature led to a lower heating capacity and a higher *COP*, and a lower normal boiling point resulted in a higher condensing pressure and evaporation

pressure. The critical temperature mainly affects the heating capacity by affecting the suction pressure of the compressor and the refrigerant density of the suction port. Therefore, to balance the heating capacity and *COP*, the alternative refrigerant needs to have a critical temperature similar to R22. The normal boiling point of the substitute refrigerant should not be excessively lower than R22, designed to avoid the excessive operating pressures of the system.

Table 4. Fundamental physical and environmental parameters.

Refrigerants	t_{nb}/°C	t_{cr}/°C	P_{cr}/MPa	ΔT/°C	ODP	GWP	Safety class
ZNM	-57.94	92.42	5.097	26.05	0	<17.7	A3
R22	-40.78	96.15	4.990	0	0.055	1600	A1

R22 had an ODP of 0.055 and a GWP of 1600, so the use of R22 caused great damage to the ozone layer and contributed to global warming. ZNM, with zero ODP and extremely low GWP, was the eco-friendly refrigerant. R22 was a synthetic refrigerant, while R744 and R290 were natural refrigerants, which can be extracted from the atmosphere, natural gas or industrial waste gas. Thus, the production of R22 required more energy and emitted more greenhouse gases. R744, R290 and R22 all had the toxicity of A in ANSI/ASHRAE 34, and none of them had an effect on human health. As a result, the use of ZNM instead of R22 was in line with the requirements of international environmental policies such as the Kigali Amendment, Paris climate agreement. ZNM was a flammable refrigerant, and its charge amount needed to be limited, but the adoption of measures such as installing the unit outdoors, installing ventilation alarm devices, setting safety walls can be significantly improve its safety, thereby increasing its charge limit and expanding its application range.

Compared with R22, ZNM had slightly lower critical temperature, markedly lower normal boiling point and larger temperature slip. This means that ZNM had the potential to replace R22 and the lower normal boiling point means that the system operating with ZNM refrigerant could obtain higher discharge pressure, suction pressure and heating capacity compared with those of system operating with R22 refrigerant. In addition, the temperature slip could enhance the heat transfer matching, thereby improving energy efficiency (*COP*) of system operating with ZNM refrigerant, which in turn reduced carbon emissions.

The saturation vapor pressure of the refrigerant is affected by the normal boiling point, critical temperature and other thermophysical properties, and it affects the operating pressure of the system. Therefore, in order to achieve drop-in replacement or minor modifications to the original system, the replacement refrigerant and R22 need to have similar saturation vapor pressure in the operating temperature zone. As illustrated in Fig. 2, the saturation vapor pressure of ZNM and R22 increased slowly at first and then rapidly with the increase of saturation temperature. The saturation vapor pressure of ZNM was slightly higher than that of R22, and the deviation between them was very small. This means that ZNM had great potential to replace R22. The latent heat of vaporization of ZNM and R22 decreased promptly with the saturation temperature increases, which was primarily owing to the marked reduction of phase transition enthalpy difference. The latent heat of vaporization of ZNM was markedly higher compared to that of R22, which means that system operating with ZNM refrigerant could obtain higher heating capacity and the optimal charge of ZNM was significantly lower than that of R22. The latter has been experimentally confirmed in our previous study [16].

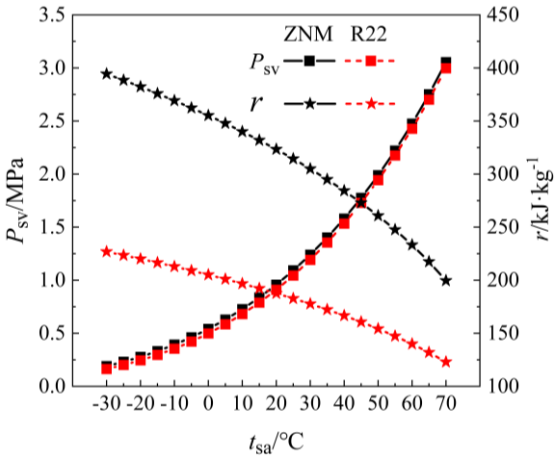

Figure 2. Saturation vapor pressure and latent heat of vaporization versus saturation temperature.

4. Results and discussion

Table 5 shows the experimental results of IHPWH operating with different refrigerants under nominal condition in this study and similar studies. The system operating with ZNM obtained the highest *COP* among them, so ZNM had remarkable alternative advantage in IHPWH system. It is worth noting that the heat sink at the gas cooler inlet was local tap water in reference [24].

Table 5. Test results of this study and similar studies.

Parameters	*COP*	P_{dis}/MPa	*r*	t_{dis}/°C	Reference
R22	4.262	1.942	3.22	95.4	This study
ZNM	4.731	2.158	2.68	69.9	This study
R744/R290 (95/5)	3.186	8.280	-	83.6	[24]
R290	4.510	1.844	2.79	71.5	[25]

4.1. Effect of ETHSK

The tap water temperature can vary markedly in different region, and that in the same region shows significant variations with the seasonal changes. Hence, the analysis and comparison of the variable ETHSK condition performances of systems operating with ZNM refrigerant and R22 refrigerant was necessary to evaluate the alternative performance of ZNM.

Figure 3(a) illustrates the variations of heating capacities and subcooling degree of condenser of systems operating with ZNM refrigerant and R22 refrigerant as a function of the ETHSK. The heating capacities of the two systems showed a different trend with the change of ETHSK. The heating capacity of system operating with ZNM refrigerant first climbed slightly and then dropped gradually as the ETHSK increased, and reached the maximum value of 5.518 kW when the ETHSK was 15 ℃. The slight increase in heating capacity of system operating with ZNM refrigerant was primarily owing to the improvement of the temperature matching level between ZNM and heat sink caused by the sluggish lift in subcooling degree of condenser and the corresponding degree of insufficient heat exchange capacity of condenser gradually decreased. The slow decrease in heating capacity of system operating with ZNM refrigerant was mainly created by the decrease of phase change condensation enthalpy caused by the rise of discharge pressure (condensation temperature) (see Fig. 4(a)) [20,26]. The heating capacity of

system operating with R22 refrigerant slowly dropped with the ETHSK increasing, primarily contributed by the decrease of phase change condensation enthalpy caused by the sluggish lift in discharge pressure. In the ETHSK range of 10~20 ℃, the heating capacity obtained by system operating with ZNM refrigerant increased by 12.79%~18.74% compared to that of system operating with R22 refrigerant, indicating that the utilization of ZNM effectively improved the heating capacity of the IHPWH. This was mainly due to the lower critical temperature (see Tab. 4) and higher latent heat of vaporization (see Fig. 2) resulting in higher heating capacity of system operating with ZNM refrigerant.

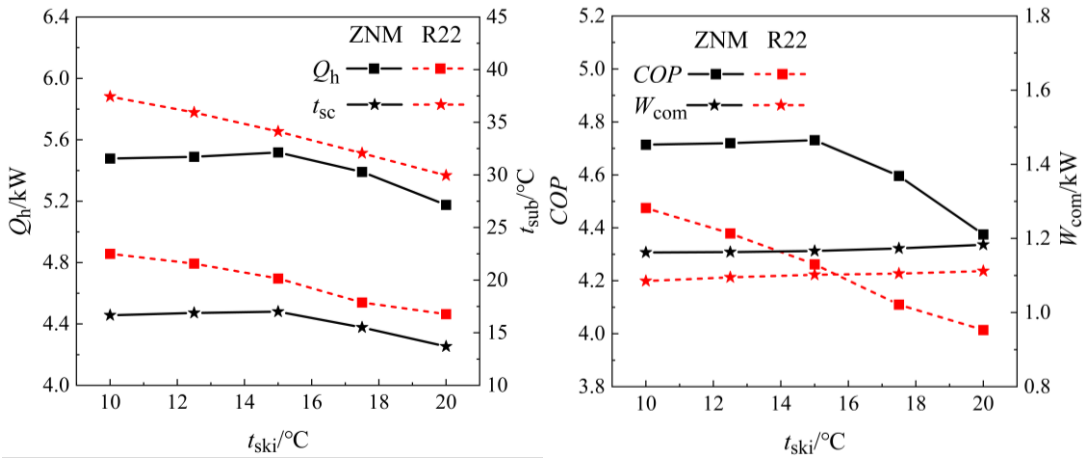

(a) (b)

Figure 3. Heating capacity, degree of subcooling, *COP* and compressor power versus ETHSK. (a) Heating capacity and degree of subcooling, and (b) *COP* and compressor power.

As presented in Fig. 3(b), the *COP*s of systems operating with ZNM refrigerant and R22 refrigerant showed a different trend with the change of ETHSK, and the variation trends of their *COP*s were similar to their corresponding heating capacities. With the rise of ETHSK, the *COP* of system operating with ZNM refrigerant first improved slightly and then reduced gradually, while system operating with R22 refrigerant obtained the approximately linearly reduced *COP*. The changes of *COP*s for the two systems were mainly the result of the joint effect of heating capacity and compressor power (see Fig. 3), in which heating capacity played a leading role. Within the ETHSK scope of 10~20 ℃, the *COP* of system operating with ZNM refrigerant was improved by 5.34%~11.82% compared with that of system operating with R22 refrigerant, mainly due to the large temperature slip of ZNM (see Tab. 4) boosted the temperature matching performance between ZNM and heat sink, and correspondingly reduced the irreversible loss of condenser. This indicated that the use of ZNM helps to improve *COP* of IHPWH system and mitigate their indirect greenhouse effect. The compressor powers of both systems increased slightly with increasing ETHSK, mainly caused by the slow augmentation of discharge pressure. Within the researchful ETHSK scope, the compressor power of system operating with ZNM refrigerant was increased by 5.81%~7.10% compared to that of system operating with R22 refrigerant.

Figure 4(a) illustrates the variations in compressor operating pressures of systems operating with ZNM refrigerant and R22 refrigerant as a function of ETHSK. As the ETHSK rose, both systems obtained the slow-rising discharge pressures, which was primarily due to the fact that the rise of ETHSK resulted in a slow lift of condensation temperature at the same OTHSK. The discharge pressure of system operating with ZNM refrigerant was increased by 0.217~0.234 MPa than that of system operating with R22 refrigerant within the ETHSK range of 10~20 ℃, but the pressure was still in the

safe operating range. Thus, there was no the risk with the safe operation of the system when ZNM was used instead of R22. With the lift of ETHSK, the suction pressures of both systems reduced slightly with a little change, mainly because of the little change in evaporator side conditions caused by the similar heat source side condition. The suction pressure of system operating with ZNM refrigerant was 0.181~0.221 MPa higher compared to that of system operating with R22 refrigerant within the ETHSK range of 10~20 ℃, and the suction pressures of both were markedly higher than the atmospheric pressure, which could avoid the safety hazard of air entering the system. The main reason that system operating with ZNM refrigerant achieved slightly higher discharge and suction pressures than those of system operating with R22 refrigerant was that ZNM had a lower normal boiling point (see Tab. 4) and a slightly higher saturation vapor pressure (see Fig. 2).

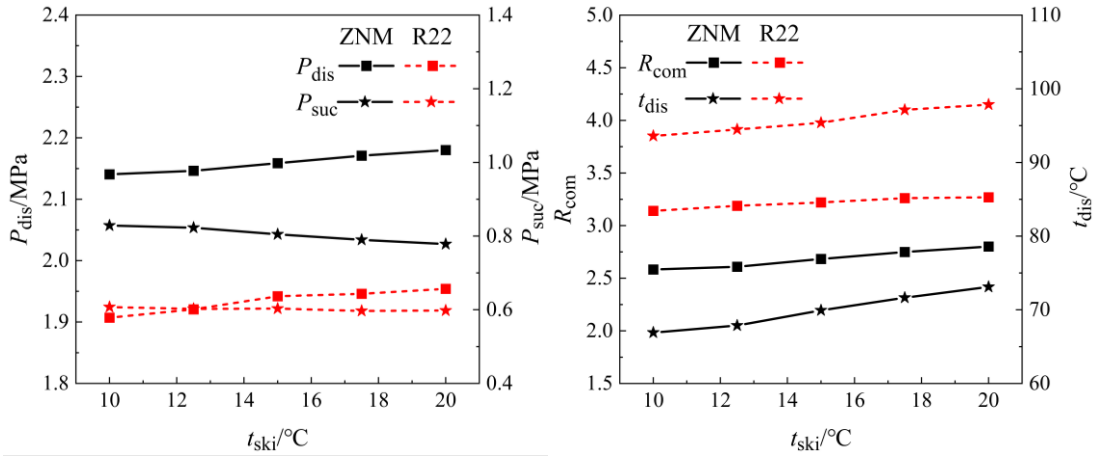

(a) (b)

Figure 4. Compressor operating parameters versus ETHSK. (a) Operating pressures, and (b) pressure ratio and discharge temperature.

Figure 4(b) depicts the impacts of ETHSK on the pressure ratios and discharge temperatures of systems operating with ZNM refrigerant and R22 refrigerant. With the lift of ETHSK, both systems achieved the slow increasing pressure ratios. The main reason was that the lift of ETHSK led to a slow rise in the discharge pressure and a slow reduction in the suction pressure. The pressure ratio of system operating with ZNM refrigerant was markedly lower than that of system operating with R22 refrigerant when the ETHSC was in 10~20 ℃, mainly because of higher suction pressure of the former caused by its lower normal boiling point and slightly higher saturation vapor pressure. The discharge temperatures of both systems tended to rise slowly as the ETHSK increased, primarily attributed to the slow growth of the pressure ratios. Within the researchful scope of ETHSK, the discharge temperature of system operating with ZNM refrigerant was markedly lower compared with that of system operating with R22 refrigerant, with a reduction of 24.8~26.7 ℃, mainly because of the former obtained the markedly lower pressure ratio. Thus, the application of ZNM enabled the IHPWH to produce hot water at the higher temperature.

4.2. Effect of ETHSC

The ETHSC is markedly influenced by season, climate type and heat source type. Therefore, it is vitally important to compare and analyze the performances of systems operating with ZNM refrigerant and R22 refrigerant under variable ETHSC condition.

Figure 5(a) reveals the effects of ETHSC on the heating capacities of systems operating with ZNM refrigerant and R22 refrigerant. The heating capacities of both systems showed a slightly different trends with the change of ETHSC. With the rise of ETHSC, the heating capacity of system operating with ZNM refrigerant rised rapidly and then slowly. The rapid rise of heating capacity was primarily owing to the rapid lift in the refrigerant mass flow brought about by the rise of suction pressure/evaporating temperature (as listed in Fig. 6(a)), while the slow rise of heating capacity was mainly due to the combined effect of the rapid decrease of phase change condensation enthalpy caused by the rapid increase of discharge pressure and the rapid increase of refrigerant flow caused by the rapid increase of suction pressure (see Fig. 6(a)). The heating capacity of system operating with R22 refrigerant increased approximately linearly and rapidly with the rise of ETHSC, which was primarily due to a quick growth of the refrigerant flow rate brought about by the increase of suction pressure. In the ETHSC range of 10~25 ℃, system operating with ZNM refrigerant obtained 4.30%~17.50% larger heating capacity than that of system operating with R22 refrigerant, mainly because of the lower critical temperature (see Tab. 4) and higher latent heat of vaporization (see Fig. 2) leading to higher heating capacity of system operating with ZNM refrigerant. When the ETHSC was 30 ℃, systems operating with ZNM refrigerant and R22 refrigerant obtained the basically equivalent heating capacity and the former was only 0.03% lower than the latter, mainly because of the apparent lack of heat transfer area of evaporator resulting in slight wet compression. It is therefore necessary and feasible to expand the heat transfer area of evaporator to improve the heating capacity of system operating with ZNM refrigerant at high ETHSC condition.

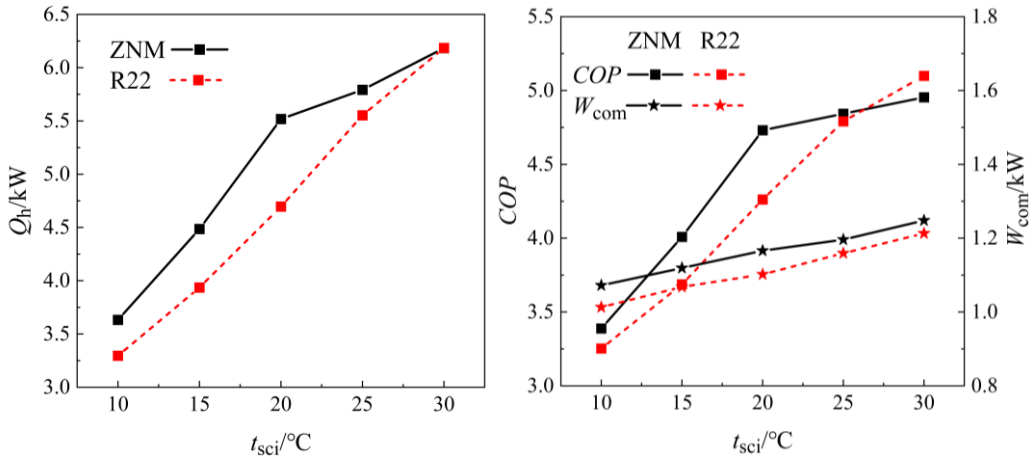

Figure 5. Heating capacity, *COP* and compressor power versus ETHSC. (a) Heating capacity, and (b) *COP* and compressor power.

As illustrated in Fig. 5(b), with the change of ETHSC, the *COP*s of the two systems had slightly different changing trends. For system operating with ZNM refrigerant, the *COP* and heating capacity had the similar changing trend. With the change of ETHSC, the *COP* of system operating with ZNM refrigerant rised rapidly first and then gently, while the *COP* of system operating with R22 refrigerant rised rapidly, which was mainly attributed to the comprehensive action of the heating capacity and compressor power, in which the heating capacity occupied a dominant position. The *COP* of system operating with ZNM refrigerant was superior to that of system operating with R22 refrigerant within the ETHSC scope of 10~25 ℃, increasing by 1.09%~11.00%, mainly due to the large temperature slip of

ZNM (see Tab. 4), which enhanced the temperature matching performance, thereby reducing the irreversible losses in the condenser and enhancing system *COP*. When the ETHSC was 30 ℃, the *COP*s of both systems operating with ZNM refrigerant and R22 refrigerant were basically equivalent, and the former was only 2.84% lower than the latter, mainly caused by the lower heating capacity and higher compressor power of system operating with ZNM refrigerant. With the increase of ETHSC, the compressor powers of both systems exhibit a sharp upward trend, primarily due to the quick rise of refrigerant flow rate brought about by the corresponding lift in suction pressure. Compared with that of system operating with R22 refrigerant, the compressor power of system operating with ZNM refrigerant was increased by 2.89%~5.82% under the variable ETHSC condition.

Figure 6(a) displays the impact of ETHSC on the compressor operating pressures of systems operating with ZNM refrigerant and R22 refrigerant. With the lift of ETHSC, the discharge pressure of system operating with ZNM refrigerant increased gently first and then rapidly, while that of system operating with R22 refrigerant increased gently. The slow rise of discharge pressures were mainly due to the heat exchange area of the condenser was sufficient and the gradually increasing accumulation of refrigerant in the condenser slowly reduced its effective heat exchange area, while the rapid rise of discharge pressure was mainly due to the heat exchange area of the condenser was insufficient at this time, and the gradually increasing accumulation of refrigerant in the condenser rapidly reduced its effective heat exchange area [27]. In the ETHSC scope of 10~30 ℃, the discharge pressure of system operating with ZNM refrigerant was increased by 0.217~0.314 MPa compared with that of system operating with R22 refrigerant, which was within the safe range, so it was unnecessary to pay excessive attention to the safety problem caused by the operating pressure. The suction pressures of both systems increased rapidly with the rise of ETHSC, mainly because the increase of ETHSC led to the rapid lift of evaporation temperature. Within the researchful ETHSC scope, the suction pressure of system operating with ZNM refrigerant was 0.100~0.283 MPa higher than that of system operating with R22 refrigerant. Furthermore, both systems exhibited the suction pressures that were distinctly higher than the atmospheric pressure, thus avoiding the safety risks of negative pressure operation. The lower normal boiling point (see Tab. 4) and slightly higher saturated vapor pressure (see Fig. 2) were the main reasons for the system operating with ZNM refrigerant to obtain slightly higher discharge and suction pressure.

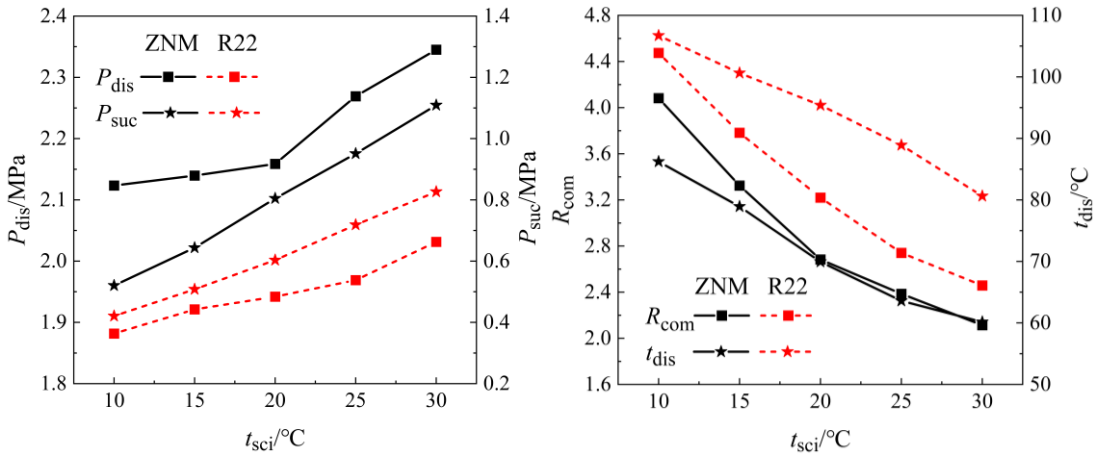

Figure 6. Compressor operating parameters versus ETHSC. (a) Operating pressures, and (b) pressure ratio and discharge temperature.

Figure 6(b) demonstrates the influence of ETHSC on pressure ratios and discharge temperatures of systems operating with ZNM refrigerant and R22 refrigerant. The pressure ratios of both systems presented trends of rapid decrease with the rise of ETHSC, mainly because the lift rate of suction pressure was markedly faster than that of discharge pressure (see Fig. 6(a)). Under the variable ETHSC condition, the pressure ratio of system operating with ZNM refrigerant was markedly lower than that of system operating with R22 refrigerant, mainly due to the much higher suction pressure of the former caused by its lower normal boiling point and slightly higher saturation vapor pressure. The discharge temperatures of both systems reduced rapidly with the lift of ETHSC, primarily attributed to the rapid decline of pressure ratios. The discharge temperature of system operating with ZNM refrigerant was reduced by 20.5~25.5 ℃ compared with that of system operating with R22 refrigerant under the variable ETHSC condition, primarily because of the former obtained the markedly lower pressure ratio. This indicated that the use of ZNM can improve the service life of lubricating oil and compressor, and make the IHPWH system with the ability to produce higher temperature hot water.

5. Conclusions

The influences of ETHSK and ETHSC on the key performance parameters of systems operating with ZNM refrigerant and R22 refrigerant, such as heating capacity, *COP*, discharge temperature, etc., were studied by using the self-built IHPWH device, aiming to further evaluate the substitution potential of ZNM in the IHPWH. The main conclusions were as follows:

(1) Substitution potential of ZNM. Compared with those of system operating with R22 refrigerant, system operating with ZNM refrigerant obtained a rise of -0.03%~18.74% and -2.84%~11.82% in the heating capacity and *COP*, and the clearly reduced discharge temperature under the variable ETHSK and variable ETHSC conditions. And only when the ETHSC was 30 ℃, the two systems had basically equivalent heating capacity and *COP*. As a result, ZNM had clear substitution advantages in the IHPWH.

(2) Trends in key system performances. With the rise of ETHSK, the heating capacity and *COP* of system operating with ZNM refrigerant first increased slightly and then reduced rapidly, while those of system operating with R22 refrigerant reduced rapidly. However, with the rise of ETHSC, the heat capacity and *COP* of system operating with ZNM refrigerant first increased rapidly and then slowly, while those of system operating with R22 refrigerant increased rapidly. The discharge temperatures of both systems elevated slowly with the increase of ETHSK, but reduced rapidly with the increase of ETHSC.

(3) High temperature hot water production potential. Compared with that of system operating with R22 refrigerant, the discharge temperature of system operating with ZNM refrigerant was markedly reduced by 24.8~26.7 ℃ and 20.5~25.5 ℃ respectively under the variable ETHSK and variable ETHSC conditions. Thus, ZNM had clear advantages in the production of high-temperature hot water.

The future research work mainly includes: (1) An efficient and reliable fast start-up control method for IHPWH system operating with ZNM will be proposed based on the study of the effect of refrigerant migration on the start-up characteristics; (2) Research on concentration optimization of R744/R290 for heat pump and its alternative performance evaluation based on 30~40 ℃ industrial waste heat recovery will be carried out, aiming to reduce carbon emissions by improving energy utilization efficiency and realize the alternative application of green and efficient refrigerant; (3) The alternative potentials of green refrigerants such as R744/R1270, HFC/HC, HC/HC in heat pump, air conditioning

and other systems will be evaluated. These studies will provide reliable data for the development and promotion of green and efficient heat pumps and air conditioners.

Acknowledgment

This work was sponsored by the National Natural Science Foundation Program of China (No. 52076219), Key Research and Development Project of Henan Province (No. 221111320200 and 231111320900), Henan Youth Science Foundation Project (No. 212300410317), Zhongyuan University of Technology Youth Talent Innovation Ability Fund Project (No. K2020QN013).

Nomenclature

c	–	specific heat [kJ·kg^{-1}·K^{-1}]	p	–	pressure
COP	–	coefficient of performance	sa	–	saturation
M	–	mass flow [kg·s^{-1}]	sc	–	heat source
P	–	pressure [MPa]	sci	–	heat source inlet
Q	–	heating capacity [kW]	sk	–	heat sink
r	–	latent heat of vaporization [kJ·kg^{-1}]	ski	–	heat sink inlet
R	–	pressure ratio	sko	–	heat sink outlet
T	–	temperature [℃]	suc	–	compressor suction
W	–	power dissipation [kW]	sv	–	saturation vapor
Greeksymbols			**Abbreviations**		
ΔT	–	temperature slip [℃]	GWP	–	Global Warming Potential
Subscripts			ETHSC	–	Entry Temperature of Heat Source
com	–	compressor	ETHSK	–	Entry Temperature of Heat Sink
cr	–	critical	OTHSK	–	Outlet Temperature of Heat Sink
dis	–	compressor discharge	IHPWH	–	Instant Heat Pump Water Heater
h	–	heating	ODP	–	Ozone Depletion Potential
nb	–	normal boiling	ZNM	–	Zeotropic Natural Mixture

References

[1] Liu, J., *et al.*, A novel two-stage compression air-source heat pump cycle combining space heating, cooling, and domestic hot water production, *Energy and Buildings*, *285* (2023), 112863

[2] Zhao, W. K., *et al.*, Decarbonization performances of a transcritical CO_2 heat pump for building heating: A case study, *Energy and Buildings*, *289* (2023), 113052

[3] Secretariat O. *The Montreal protocol on substances that deplete the ozone layer*, United Nations Environment Programme, Kigali, Rwanda, 2016

[4] Yu, J. L., *et al.*, A thermodynamic analysis of a transcritical cycle with refrigerant mixture R32/R290 for a small heat pump water heater, *Energy and Buildings*, *42* (2010), 12, pp. 2431-2436

[5] Tian, Q. Q., *et al.*, An experimental investigation of refrigerant mixture R32/R290 as drop-in replacement for HFC410A in household air conditioners, *International Journal of Refrigeration*, *57* (2015), pp. 216-228

[6] Wang, F., *et al.*, Study on performance of bifunctional heat pump systems using HFC125/HC mixtures, *Journal of the Energy Institute*, *85* (2012), 2, pp. 78-85

[7] Sieres, J., *et al.*, Drop-in performance of the low-GWP alternative refrigerants R452B and R454B in an R410A liquid-to-water heat pump, *Applied Thermal Engineering*, *182* (2020), 116049

[8] Fukuda, S., *et al.*, The circulation composition characteristic of the zeotropic mixture R1234ze(E)/R32 in a heat pump cycle, *International Refrigeration and Air Conditioning Conference*, West Lafayette, Indiana, 2012, paper. 1221

[9] Wang, Y., *et al.*, Application of environmental friendly material R32/R1234ze in heat pump water heater, *Advances in Engineering Research*, *93* (2016), pp. 420-425

[10] Yu, B. B., *et al.*, Modeling and theoretical analysis of a CO_2-propane autocascade heat pump for electrical vehicle heating, *International Journal of Refrigeration*, *95* (2018), pp. 146-155

[11] Luo, J. L., *et al.*, Performance investigation on a novel air-source heat pump using CO_2/HC for recirculated water heater in cold regions, *Sustainable Energy Technologies and Assessments*, *53* (2022), 102496

[12] Luo, J. L., *et al.*, Experimental investigations on the performance of a single-stage compound air-source heat pump using CO_2/R600a in cold regions, *Applied Thermal Engineering*, *205* (2022), 118050

[13] Liu, J., *et al.*, Performance evaluation of low GWP large glide temperature zeotropic mixtures applied in air source heat pump for DHW production, *Energy Conversion and Management*, *274* (2022), 116457

[14] Zhang, X. P., *et al.*, Determination of the optimum heat rejection pressure in transcritical cycles working with R744/R290 mixture, *Applied Thermal Engineering*, *54* (2013), 1, pp. 176-184

[15] Dai, B. M., *et al.*, Assessment of heat pump with carbon dioxide/low-global warming potential working fluid mixture for drying process: Energy and emissions saving potential, *Energy Conversion and Management*, *222* (2020), 113225

[16] Ju, F. J., *et al.*, Experimental investigation on a heat pump water heater using R744/R290 mixture for domestic hot water, *International Journal of Thermal Sciences*, *132* (2018), pp. 1-13

[17] Ju, F. J., *et al.*, Experiment and simulation study on performances of heat pump water heater using blend of R744/R290, *Energy and Buildings*, *169* (2018), pp. 148-156

[18] Cui, Q., *et al.*, Pinch point characteristics and performance evaluation of CO_2 heat pump water heater under variable working conditions, *Applied Thermal Engineering*, *207* (2022), 118208

[19] Pitarch, M., *et al.*, Experimental study of a subcritical heat pump booster for sanitary hot water production using a subcooler in order to enhance the efficiency of the system with a natural refrigerant (R290), *International Journal of Refrigeration*, *73* (2017), pp. 226-234

[20] Pitarch, M., *et al.*, Exergy analysis on a heat pump working between a heat sink and a heat source of finite heat capacity rate, *International Journal of Refrigeration*, *99* (2019), pp. 337-350

[21] GB/T 23137-2020, Heat pump water heat for household and similar application, General administration of quality supervision, Inspection and Quarantine of the People's Republic of China, Standardization Administration of the People's Republic of China, Beijing, China, 2020.

[22] Li, T. X., *et al.*, High temperature hot water heat pump with non-azeotropic refrigerant mixture HCFC-22/HCFC-141b, *Energy Conversion and Management*, *43* (2002),15, pp. 2033-2040

[23] Moffat, R. J., *et al.*, Describing the uncertainties in experimental results, *Experimental Thermal and Fluid Science*, *1* (1988),1, pp. 3-17

[24] Zhang, X. P., *et al.*, An investigation of heat pump system using CO_2/propane mixture as a working fluid, *International Journal of Green Energy*, *14* (2016), pp. 105-111

[25] Huang, Y. Y., *et al.*, Experimental study and comparison of R290 air source heat pump water heater (in Chinses), *Refrigeration and Air-conditioning*, *3* (2011), pp. 57-60

[26] Pottker, G., Hrnjak, P., Effect of the condenser subcooling on the performance of vapor compression systems, *International Journal of Refrigeration*, *50* (2015), pp. 156-164

[27] Corberán, J. M., *et al.*, Influence of the source and sink temperatures on the optimal refrigerant charge of a water-to-water heat pump, *International Journal of Refrigeration*, *34* (2011), 4, pp. 881-892.

Submitted: 25.01.2024.
Revised: 25.08.2024.
Accepted: 28.08.2024.